

## ON CATALOGUE OF GEOSTATIONARY SATELLITES

K.V.Grigoriev, A.S.Sochilina, A.N.Vershkov

Institute of Theoretical Astronomy, RAS, St.Petersburg

### ABSTRACT

The description of the dynamics of objects in or near the geostationary ring can be simplified by introducing the Laplacian plane. On the base of this plane the first order theory was developed, which includes perturbations from the geopotential ( $l=6$ ), luni-solar attraction and a simplified model for radiation pressure. The theory was applied to the data of uncontrolled geostationary objects gathered by several national cosmic centres.

The catalogue containing orbital elements of uncontrolled objects in or near the geostationary ring is now available. It is based on initial elements provided by ESOC and makes use of the theory of motion developed at ITA. Parameters listed in the catalogue allow predicting ephemerides of any objects over 100 to 200 days.

### 1. INTRODUCTION

The remarkable property of geostationary satellites (GS) is the commensurability of their motion with the Earth's rotation, like 1:1, which has led to the intensive use of them in satellite communication systems.

During 30 years the geostationary orbit (GEO) has been filled up with a such number of various objects, that a hazard of their collisions has become real. Now, this problem is a rather sharp, because geostationary objects are fated to be eternal and the launch of GS is in progress (Refs. 1-2).

Namely this circumstance attracts specialists to the solution of GEO problem: the investigations of the variety of GS motions with the aim to select the conditions of optimal launches of satellites and their further exploitation. The investigations of GS orbital evolution help us to determine the region of their distribution and, consequently, the region, where the small debris can be looked for. Therefore, in the first place a catalogue of orbits has to be compiled for all GS, which can be observed in GEO and in its vicinities, by optical means only. Such catalogue should contain the orbital information for observers and analysts, permitting to compute ephemerides and to identify the objects.

For organization of such catalogue and its support one can use the experience of work with natural bodies, for instance, the observation service of minor planets. This work is already being carried out for two centuries and

now the service of minor planets deals with more than five thousands of asteroids.

The orbital data, accumulated by national space research centres during 30 years in spite of their poor accuracy, have to be used as a basis of such catalogue. At last, the activity of the participants of scientific programs "COGEOS" and "Stationar-equator", their experience in work with collected precise observations also have to be taken into account. An analog of a such catalogue has been formed in ITA RAS on the base of the last seven LOG issues of ESOC (Ref. 3), which contains the orbital data for 1992 year.

In this catalogue the results of the ESOC data comparisons and computations on the base of GS motion theory, developed at ITA, have been given. The classification of GS has been done according to their motion. For all GS the values of the resonant periods of librations have been determined and the improved values of GS drift rates have been calculated on base of known longitudes. It is proposed that the catalogue and the PC-oriented software produced in ITA (Refs. 4-5), will help the observers and analysts who need calculate ephemerides, predict conditions of visibility of GS and identify the objects.

### 2. THEORETICAL FOUNDATION OF CATALOGUE

#### 2.1 The choice of the coordinate system

The quality of the theory of a celestial body orbital motion depends on the choice of a coordinate system. For the study the Earth's satellite motion the system proposed by Kozai (Ref. 12) has been adopted, in which inclination ( $i$ ) and argument of perigee ( $\omega$ ) of the orbit are referred to the equator of date, and the longitude of ascending node  $\Omega$  is measured from a fixed point along a fixed plane and then along the equator of date.

This coordinate system is not appropriate for GS because of nonlinear changes in the inclination and the node due to the influence of the luni-solar perturbations. In the similar case for the study of the natural satellite motion the Laplacian plane is adopted as the reference plane.

The Laplacian plane is a plane relative to which the compensation of main perturbations due to the planet's oblateness and the attraction of the third body takes place. This plane is inclined to the equator of date at a certain angle  $\Lambda$  and passes through the fixed equinox (Ref. 6). The value  $\Lambda$  is determined from the following equation :

$$tg2\Lambda = \frac{\kappa_1 \sin 2\varepsilon}{2j_{20}(a_e/a)^2 n^2 + \kappa_1 \cos 2\varepsilon} \quad (1)$$

where  $\kappa_1 = \kappa(1 - 15/8e^4 + O(e^6))$ ,  $\kappa$  is the constant, which depends on orbital elements of the Moon and the Sun,  $\varepsilon$ =inclination of ecliptic to the equator of date,  $j_{20} = -\sqrt{5C_{20}}$  is parameter of the geopotential,  $a_e$  =the Earth's mean equatorial radius,  $a, e, n$  = orbital elements of GS: semi-major axis, eccentricity and mean motion .

For different objects on GEO the value of  $\Lambda$  can vary within of the limits  $5.8^\circ < \Lambda < 8.0^\circ$ . Below the formulae for the transition to the Laplacian plane of the orbital elements referred to the equator are given:

$$\begin{aligned} \sin i_\Lambda \sin \Omega_\Lambda &= \sin i \sin \Omega \\ \sin i_\Lambda \cos \Omega_\Lambda &= -\cos i \sin \Lambda + \sin i \cos \Lambda \cos \Omega \\ \cos i_\Lambda &= \cos i \cos \Lambda + \sin i \sin \Lambda \cos \Omega \\ \sin i_\Lambda \sin d &= -\sin \Lambda \sin \Omega \\ \sin i_\Lambda \cos d &= \sin i \cos \Lambda - \cos i \sin \Lambda \cos \Omega \\ \omega_\Lambda &= \omega + d. \end{aligned} \quad (2)$$

## 2.2 The principal perturbing forces.

The following forces act on the motion of the GS and evolution of these objects: the Earth's gravitational field, luni-solar perturbations and solar radiation pressure.

The expression of the geopotential, in which the orbital elements are referred to the Laplacian plane has the following form (Ref. 7):

$$\begin{aligned} U &= \text{Re} \frac{GE}{a} \sum_{l=2}^6 \sum_{m=-l}^l \sum_{k=-l}^l \sum_{p=0}^q G_{lm}^* E_{lmk}(\Lambda) \\ &\times D_{lkp}(i_\Lambda) X_{l-2p+q}^{-l-1, l-2p}(e) \exp \sqrt{-1} \psi_{lmkpq} \end{aligned} \quad (3)$$

where

$$\begin{aligned} G_{lm}^* &= (-1)^m (\sqrt{-1})^{l+m} \bar{G}_{lm} (a_e/a)^l, \\ \psi_{lmkpq} &= (l-2p)\omega_\Lambda + (l-2p+q)M + k\Omega_\Lambda - m\theta, \\ M &- \text{mean anomaly, } GE = \text{gravitational constant multiplied} \\ &\text{by the mass of the Earth, } \theta = \text{right ascension of Greenwich,} \\ \bar{G}_{lm} &= \bar{C}_{lm} - \sqrt{-1} \bar{S}_{lm}, \quad \bar{C}_{lm}, \quad \bar{S}_{lm} - \text{parameters of the} \\ &\text{geopotential, } D_{lkp}(i_\Lambda), \quad E_{lmk}(\Lambda) = \text{inclination functions} \end{aligned}$$

and  $X_{l-2p+q}^{-l-1, l-2p}(e)$  - Hansen coefficients have been given in Ref. 8.

It should be noted that in this development of  $U$  an extra summation over index  $k$  has been introduced, therefore in the argument  $\psi_{lmkpq}$  there is present the node  $\Omega_\Lambda$ .

For satisfactory precision it is sufficient to take into account the Hill's term or term with index  $l=2$  only in the development of luni-solar perturbations. Then the lunar function  $R_L$  can be expressed as:

$$\begin{aligned} R_L &= \text{Re} \frac{Gm_L}{5a} \sum_{m=0}^l \sum_{k=-1}^l \sum_{p=0}^l \sum_{p'=0}^l \sum_{q=-1}^l \sum_{q'=-1}^l B_L \times \\ &\times E_{lmk}(\varepsilon - \Lambda) D_{lkp}(i_\Lambda) X_{l-2p+q}^{l-1, l-2p}(e) \exp \sqrt{-1} \psi, \quad (4) \\ B_L &= (-1)^k \left( \frac{a}{a_L} \right)^{l+1} D_{l-mp}(i_L) X_{l-2p+q}^{-l-1, l-2p}(e_L), \end{aligned}$$

where

$$\begin{aligned} \psi &= (l-2p)\omega_\Lambda + (l-2p+q)M + k\Omega_\Lambda \\ &+ (l-2p'+q')M_L + (l-2p')\omega_L - m\Omega_L. \end{aligned}$$

The Sun's perturbation function has the same form but instead of index  $L$ (lunar), there will be  $S$ (Sun). The third Kepler's law for both bodies is adopted as:

$$G(E+m) = n_L^2 a_L^3,$$

$$G(E+m_S+m_L) = n_S^2 a_S^3.$$

Now if we collect all the terms with the argument  $\Omega_\Lambda$  from functions  $U, R_L, R_S$  we shall obtain:

$$\begin{aligned} U_\Omega &= \frac{3}{8} a^2 \sin 2i_\Lambda \cos(\Omega_\Lambda) \\ &\times \left\{ \kappa \left( 1 + \frac{3}{2} e^2 \right) \sin 2(\varepsilon - \Lambda) - 2J_{20} \left( \frac{a_e}{a} \right)^2 n^2 (1 - e^2)^{\frac{3}{2}} \sin 2\Lambda \right\} \quad (5) \end{aligned}$$

where

$$\begin{aligned} \kappa &= n_L^2 \mu_L (1 - e_L^2)^{-3/2} \left( 1 - \frac{3}{2} \sin^2 i_\Lambda \right) + n_S^2 \mu_S (1 - e_S^2)^{-3/2}, \\ \mu_L &= \frac{m_L}{E + m_L}, \quad \mu_S = \frac{m_S}{m_S + E + m_L}. \end{aligned}$$

From the equation  $U_\Omega = 0$  one obtains the formula (1) for determining the angle  $\Lambda$ . It should be noted that both derivatives  $dU_\Omega/da$  and  $dU_\Omega/de$  are not equal to zero, but in the GS case the last derivative is rather negligible.

For taking into account the influence of the solar radiation pressure the theory by Kozai (Ref. 9) can be used but only with orbital elements of GS referred to the Laplacian plane and with  $\varepsilon$  changed to  $\varepsilon - \Lambda$ .

## 2.3 The evolution of orbits and classification of GS

The introduction of the Laplacian plane allows to decrease interactions between different perturbations and to obtain by a classic method the luni-solar and radiation pressure perturbations in orbital elements, using the Lagrange's equations.

The radiation pressure causes the periodic variations of  $e$ ,  $\omega$  and  $M$ , but  $\delta(\omega+M)=0$ . For GS these perturbations for usual objects are significant only if the precise observations are used.

The luni-solar perturbations do not contain the term with argument  $\Omega_\Lambda$  in all elements except in mean anomaly  $M$  as follows from Eq.(5):

$$\begin{aligned} dM/dt = & -\frac{15}{4} J_{20} (a_e/a)^2 n \sin 2\Lambda \\ & \times \sin 2i_\Lambda \cos \Omega_\Lambda (1-e^2)^{-3/2} \end{aligned} \quad (6)$$

In this equation  $i_\Lambda$  is nearly constant and  $\Omega_\Lambda$  is a linear function of time. Therefore, for integrating the equation (5) it is necessary to find secular perturbations from the geopotential and the luni-solar attraction. Their expressions have the same classical forms but the factors  $(1-3/2 \sin^2 \Lambda)$  for the geopotential and  $(1-3/2 \sin^2 (\varepsilon - \Lambda))$  for luni-solar attraction appear.

The tesseral and sectorial harmonics of the geopotential cause the main resonant perturbations in the longitude  $\lambda = M + \omega + \Omega - \theta$  and in the semimajor axis  $a$  because of commensurability between  $\dot{\lambda}$  and  $\theta$  ( $l-2p+q = m$ ). In this case  $\dot{\lambda}$  becomes a variable, and the equation for  $\ddot{\lambda}$  according to (Refs. 10-11) assumes the following form:

$$\begin{aligned} \ddot{\lambda} + n^2 \sum A_{lmkpq} \sin(m\lambda - m\lambda_{lmkpq} + (k-m)\Omega_\Lambda) &= \text{LSP}, \\ \dot{a} = -\frac{3a}{2n} \ddot{\lambda}, \end{aligned} \quad (7)$$

where

$$\begin{aligned} A_{lmkpq} &= 3m(a_e/a)^l \bar{J}_{lm} Q_{lmkpq}, \\ Q_{lmkpq} &= D_{lpq}(i_\Lambda) E_{lmk}(\Lambda) X_{l-2p+q}^{-l-1, l-2p}(e), \\ \bar{C}_{lm} &= \bar{J}_{lm} \cos m\lambda_{lm}, \quad \bar{S}_{lm} = \bar{J}_{lm} \sin m\lambda_{lm}, \\ m\lambda_{lmkpq} &= m\lambda_{lm} + q\omega_\Lambda \\ &= \begin{cases} (1+\xi)\pi/2, & \text{if } \begin{cases} l-m & \text{even} \\ l-m & \text{odd} \end{cases} \\ \xi\pi/2 \end{cases} \\ \xi &= \begin{cases} +1 \\ -1 \end{cases} \text{if } \left\{ (-1)^{E(l+m+1)/2} Q_{lmkpq} \right\} \begin{cases} < 0 \\ > 0 \end{cases} \end{aligned}$$

The right-hand side of the equation (8) LSP consists of the luni-solar perturbations:

$$\begin{aligned} \text{LSP} = & 15/4 (a_e/a)^2 j_{20} (1-e^2)^{-3/2} \dot{\Omega}_\Lambda \sin 2\Lambda \\ & \times \sin 2i_\Lambda \sin \Omega_\Lambda + \frac{d}{dt} \left( \frac{d\lambda}{dt} \right)_{LS} \end{aligned} \quad (8)$$

In the Table 1. the numerical values of  $A_{lmkpq}$  and  $m\lambda_{lmkpq}$  have been given for the ordinary GS.

$lmkpq$	$(k-m)$	$A_{lmkpq} \cdot 10^6$	$m\lambda_{lmkpq} \cdot 10^6$ (rad)
2200	1	0.47	5.762
2200	0	29.14	2.620
3110	0	1.25	0.124
3300	1	0.10	1.105
3300	0	4.01	2.037
4210	0	0.14	-1.086
4400	0	0.19	-1.086

Table 1. The numerical values of  $A_{lmkpq}$  and  $m\lambda_{lmkpq}$  for GS with  $i_\Lambda = 7.0215$ .

The value of LSP is rather small and the amplitude of the main term does not exceed  $0.2 \cdot 10^{-8}$ , therefore, in many cases it can be neglected. From Table 1. it can be seen that the terms with  $\Omega_\Lambda$  have the amplitude no more than  $0.47 \cdot 10^{-6}$ . On the interval of 200 days changes of  $\Omega_\Lambda$  amount to  $3.07$ , that corresponds to the change of coefficient  $A_{lmkpq}$  by  $0.03 \cdot 10^{-6}$ . Such value can be due to the errors of the geopotential parameters. Therefore the equation (7) with LSP=0 may be considered as a resonant equation with a slowly changing parameter  $\Omega_\Lambda$  ( $\dot{\Omega}_\Lambda = -0.00185/\text{day}$ ), and the solution of (7) for some time interval can be written as:

$$\begin{aligned} \dot{\lambda}^2 &= C - W(\lambda), \\ W(\lambda) &= -2 \sum A_{lmkpq} \cos(m\lambda - m\lambda_{lmkpq} + (k-m)\bar{\Omega}_\Lambda) / m, \quad (9) \\ a &= a_0 - \frac{2a}{3n} \dot{\lambda}, \end{aligned}$$

where  $\bar{\Omega}_\Lambda$  is the mean value of node on this time interval.

In the theory of nonlinear oscillations the constant  $C$  is called the total energy of the system and defined by initial values of  $\lambda$  and  $\dot{\lambda}$  at some moment of time  $t_0$ ,  $\dot{\lambda}^2/2$  - kinetic energy,  $W(\lambda)/2$  = potential energy. When  $\dot{\lambda} = 0$ , the borders of oscillations can be defined ( $\lambda_b$  and  $\lambda_e$ ) from the equation  $W(\lambda) = C$ . Then period of libration  $P$  will be determined as:

$$P = 2 \int_{\lambda_b}^{\lambda_e} \frac{d\lambda}{\sqrt{C - W(\lambda)}}.$$

For the circulation the period of oscillation will be have the same expression, only  $\lambda_b = \lambda_0$  and  $\lambda_e = \lambda_0 + \pi$ . In Figure 1. the shape of the curve  $W(\lambda)$  and the phase plane in coordinates  $\lambda, \dot{\lambda}$  for different levels  $C$  are represented.  $W(\lambda)$  has two minima (stable points of equilibrium: L1 =  $75^\circ$  E and L2 =  $105^\circ$  W) and two maxima (unstable points:

L3= 161° E and L4=15° W). The  $W(\lambda)$  and the value of  $C$  permit to classify different kinds of motion.

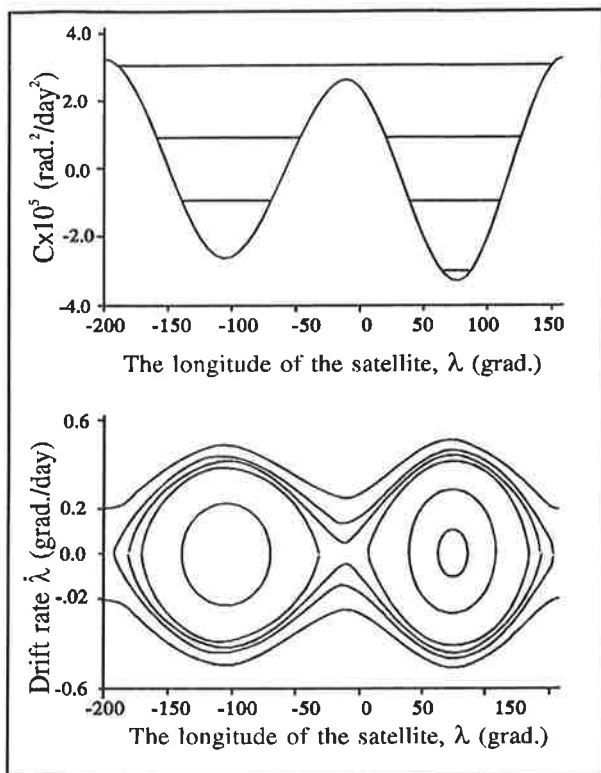


Figure 1. The curve  $W(\lambda)$  and phase plane  $\lambda, \dot{\lambda}$  for different levels of  $C$ .

In the catalogue the following classification for the GEO objects is adopted:  $l1$ = motion around L1;  $l2$ = that around L2;  $l3$ = that around both points;  $d1$ =circular motion with  $|\dot{\lambda}| < 2.05$ ;  $d2$ = circular motion with  $|\dot{\lambda}| < 12.05$ ;  $d3$ :  $|\dot{\lambda}| > 2.05$ . This classification is used in calculation of resonant perturbations.

### 3. THE ANALYSIS OF CATALOGUE DATA

The principal aim of this work is to create a catalogue of orbital data, which will be valid for a long time in predicting the ephemerides. This task can be solved in two ways. The first way is the determination of orbits on the base of precise observations. Another one is the use of orbital data, obtained by Space Research Centres. However, it turned out that both ways are quite compatible, but the last one is more simple.

The European Space Operations Centre (ESOC) has kindly provided us for the orbital data for this experiment. All objects have been separated into some groups in accordance with 2.3. The angle  $\Lambda$  has been determined for each object and orbits have been referred to their own Laplacian plane. The data from the first issue (it does not always coincide with the first LOG issue) have been taken for the initial ones and their evolutions have been computed. Because of a low precision of the rate of drift

$\dot{\lambda}$  this element had to be improved. In most of cases the accuracy of the orbital elements is quite satisfactory.

In Table 2. the orbital data of GS 84 16A Raduga 14 from the catalogue have been represented. After the line with the name of GS and its type ( $l1$ ) there are seven lines with ESOC orbital elements referred to the Laplacian plane and to equator. Then the line follows with different values: the period of libration  $P=748.01$  (days), the inclination of the Laplacian plane to equator  $\Lambda=7.0343701$ , mean value of eccentricity  $e=0.000903$ ,  $\dot{\lambda}=0.04813/\text{day}$  ( $\dot{\lambda}=360/P$ ),  $C=0.302659 \cdot 10^{-4}$ .

In the next eight lines (instead of seven, because GS passes  $\lambda_b=63.013$  during this time interval) the evolution of the orbit according to the theory motion has been given. In the intermediate lines the discrepancies between ESOC data and the evolution have been represented.

In the last three lines the predictions of the orbital data for moments of time, on which GS will pass the borders libration  $\lambda_b, \lambda_e$  and  $\lambda=l1$ , have been given.

The improved elements of GS 84 16A at  $T_0=48897.960279$  have been obtained by using of the precise observations (Gissar observatory). In Table 3. the ESOC orbits and the results of the evolution of the improved orbit, referred to equator have been represented.

The comparison of these data allows to estimate the accuracy of ESOC orbits.

We estimate the precision of each orbit as follows: inclinations  $\pm(0.001-0.003)$ , longitude  $\pm(0.005-0.02)$ , node  $\pm(0.01-0.02)$ , rate of drift  $\pm 0.001$ . The accuracies of argument perigee and eccentricity are very poor and it is very difficult to notice any influence of radiation pressure. In future nonsingular variables have to be introduced to improve their precision.

After smoothing out the orbital elements and improving the rate of drift, they can be used on a long interval. Therefore, according to these data the evolutions of orbits has been computed.

The reliability of these evolutions for some objects has been checked by backward evolutions and comparisons with observational data. Not all objects, however, have satisfactory orbits. Part of them (the list is added to catalogue) was not observed for more than twenty years. Some objects have only one or two orbits. Finally in accordance with a method of computation, all the objects were divided into two group.

The objects with circular motion ( $|\dot{\lambda}| > 2.05$ ) enter the first group. The drift of these satellite is quite stable and has some small oscillations which have to be averaged on the long intervals of time, taking into account Eq. (9). These oscillations are due to resonant harmonics of the geopotential and at longitudes  $30^\circ, 120^\circ, 210^\circ$  and  $300^\circ$

the rate of drift coincides with the mean value of  $\dot{\lambda} = 360^\circ / P$ .

It can be shown that for objects of the first group the motion theory can be applied on interval more than 20 years to represent the orbital data, obtained by space centres.

Table 4. gives the results of comparison of GS 67 66 C (ESOC-E and NASA-N data) with its evolution (ITA). It is not the ordinary case, because there are some errors of identifications in these data. It becomes clear when the evolution of  $i_\Lambda$  and discrepancies in  $\Delta\lambda$  are treated. In the column  $\Delta\lambda_s$  the discrepancies for short interval are given.

The possible cause of the uncorrected identification is that the orbit could be determined by observations belonging to different satellites. The objects with drift:  $\dot{\lambda} < 2.05$  represent the second group. In this group the main attention is paid to taking into account the resonant perturbations. Here we have two kinds of motion: libration and circulation. To represent longitudes  $\lambda$  obtained for different moments of time it is necessary to have a precise initial value of the drift  $\dot{\lambda}$ , and the limit of oscillations.

Due to the change of  $\Omega_\Lambda$  the potential energy of system  $W(\lambda)$  also changes with the period equal to 54 years and it causes a displacement of the whole curve  $W(\lambda)$  (Fig.1) along the abscissa  $\lambda$  as follows:

$$d\lambda/d\Omega_\Lambda = 0.4^0 \cos(2\lambda - 330^\circ - \Omega_\Lambda)$$

Besides, the deformation of  $W(\lambda)$  occurs. Probably this phenomenon explains the passages of some GS from the libration into the circulation mode. For instance, 15 year ago GS 67 01A Intelsat 2F-2 was moving around both points of librations (I3), but now, according ESOC data, it passed the unstable point 161° E instead of revolving about it.

#### 4. CONCLUSIONS

1. This GS catalogue has become possible due to cooperation of ESOC and ITA. The analysis on many uncontrolled motion objects for nearly one year, has proved, that it is preferable to determine the orbital elements with observations distributed over long time as GS. In these cases the orbits are more reliable and probability of GS loss is negligible.

2. The catalogue is not now completed because of lack of new orbital data for many GS. Therefore the activity has to be undertaken for searches of these data and probably for organizing of their observations.

3. The GS evolution is mostly due to the gravitational forces and it is very complicate. Therefore, the precise observations are very useful in these investigations. It is very important to gather all the precise observations and after identifications to publish. The national space centres

have to support this work. The available GS catalogue, software and observations will allow to concentrate all the efforts in studies of geostationary ring.

#### 5. ACKNOWLEDGMENTS

The activity and help in the organization of this work by Walter Flury and the regular preparation of LOG issues by Guy Janin have been much appreciated by authors.

#### 6. REFERENCES

1. Space Debris. The report of the ESA Space Debris, Working group, ESA-SP 1109, 469-476, 1988.
2. Flury W., Activities on Space debris in Europe, *Acta astronautica*, Vol.26, No.7, 469-476, 1992.
3. Janin G., LOG of objects near the geostationary ring, *ESOC*, No.6-12, 1992.
4. Vershkov A.N., et al., Laplace-Software for observations of geostationary objects, *Thesis of conference 'Modern methods of Phys. Geod. and Sat.Geodynamics'*, ITA, St.Petersburg, Russia, Mar.3-5, 1992.
5. Vershkov A.N. and Grigoriev K.V., Electronic catalogue of orbital elements of the geostationary satellites, *Thesis of conference 'Computers' methods of celestial mechanics'*, ITA, St.Petersburg, Russia, Nov.24-26, 1992.
6. Gayazov I.S. and Sochilina A.S., On the choice of reference frame in investigations of high satellites motion, *Bull.ITA*, Vol.15, No.9(172), 481-485, 1986.
7. Sochilina A.S., Luni-solar perturbations and motion of high satellites, *Bull ITA*, No.7 (170), 383-395, 1985.
8. Gaposchkin E.M., Smithsonian standard Earth (III), *SAO Spec.Rep.* No.353, 1973.
9. Kozai Y., Effects of solar radiation pressure on the motion of artificial satellite, *SAO Spec. Rep.*, No.56, 1961.
10. Gedeon G.S., Tesseral resonance effect on satellite orbits, *Celest.Mech.*, Vol.1, No.2, 167-189, 1969.
11. Sochilina A.S., The use of geosynchronous satellites for determining parameters of the geopotential, *Observations artificial Earth Satellites*, No.23, Publ.Astr.Inst.Czech.Academy of Sci., No.58, Praha, 211-230, 1984.
12. Kozai Y., Effect of Precession and Nutation on the Orbital Elements of a Close Earth Satellite. *Astr. Jour.*, Vol.65, No.10, 621-623, 1960.

N	Date	MJD	$i_{\Lambda}$	$\Omega_{\Lambda}$	$\omega_{\Lambda}$	$\lambda_{\Lambda}$	$\dot{\lambda}_{\Lambda}$	$i$	$\Omega$	$\omega$	$\lambda$	
40			84016A Stasionar-raduga 14				II		ESOC			
6	2/12/92	48664.578838	7. <sup>o</sup> 24	130. <sup>o</sup> 72	122. <sup>o</sup> 09	74. <sup>o</sup> 12	-1.0	6. <sup>o</sup> 07	64. <sup>o</sup> 66	189. <sup>o</sup> 3	74. <sup>o</sup> 47	
7	4/12/92	48724.428130	7.21	129.73	180.9	68.66	-1.0	6.17	63.95	247.0	69.02	
8	8/02/92	48836.133785	7.20	127.05	158.7	63.15	-.02	6.47	62.53	223.5	63.52	
9	9/03/92	48868.044704	7.18	126.22	136.2	63.26	.01	6.56	62.06	200.7	63.63	
10	10/02/92	48897.960279	7.17	125.69	138.3	63.85	.02	6.61	61.69	202.7	64.22	
11	11/23/92	48949.807063	7.16	124.49	161.5	67.06	.07	6.74	61.06	225.3	67.44	
12	1/19/93	49006.636754	7.14	123.27	180.5	71.89	.09	6.87	60.36	243.8	72.27	
748.012690			7.343701		.000903		.4813		-.302659E-04		ITA	
1	2/12/92	48664.578838	7.24	130.72	122.9	74.12	-.0965	6.07	64.66	189.3	74.47	
			.00	.00	.0	.00	.00	.00	.00	.0	.00	
2	4/12/92	48724.428130	7.23	129.47	125.2	68.66	-.0822	6.21	63.94	191.1	69.02	
			-.01	.26	55.7	.00	-.02	-.04	.01	55.9	.00	
3	8/02/92	48836.133785	7.20	127.05	129.7	63.18	-.0058	6.47	62.55	194.5	63.54	
			.00	.00	29.0	-.02	-.01	.00	-.02	29.0	-.02	
4	8/13/92	48847.688238	7.20	126.90	130.0	63.13	.0000	6.49	62.46	194.8	63.50	
5	9/03/92	48868.044704	7.19	126.53	130.6	63.29	.0141	6.53	62.25	195.3	63.66	
			-.01	-.31	5.5	-.04	.00	.03	-.20	5.4	-.03	
6	10/02/92	48897.960279	7.18	126.01	131.6	64.10	.0332	6.58	61.95	196.0	64.47	
			-.01	-.32	6.7	-.25	-.01	.03	-.26	6.6	-.25	
7	11/23/92	48949.807063	7.17	124.77	133.9	67.03	.0722	6.71	61.24	197.8	67.41	
			-.01	-.28	27.5	.03	.00	.03	-.19	27.4	.03	
8	1/19/93	49006.636754	7.15	123.58	136.1	71.82	.0937	6.84	60.57	199.5	72.20	
			-.01	-.31	44.4	.07	.00	.03	-.20	44.3	.07	
9	8/23/93	49222.534964	7.09	119.13	144.4	86.13	.0000	7.30	58.04	205.9	86.52	
10	2/25/94	49408.444467	7.03	115.32	151.6	74.69	-.0966	7.68	55.88	211.5	75.10	
11	9/01/94	49596.971991	6.97	111.49	158.9	63.13	.0000	8.05	53.73	217.0	63.55	

Table 2. The representation of the Catalogue data for 84 016A Raduga 14.

T(MJD)	$i_{ESOC}$	$i$	$\Omega_{ESOC}$	$\Omega$	$\omega_{ESOC}$	$\omega$	$\lambda_{ESOC}$	$\lambda$
48664.5788	6. <sup>o</sup> 07	6. <sup>o</sup> 07	64. <sup>o</sup> 66	64. <sup>o</sup> 59	189. <sup>o</sup> 3	213. <sup>o</sup> 2	74. <sup>o</sup> 47	74. <sup>o</sup> 46
48724.4281	6.17	6.22	63.95	63.89	247.0	211.4	69.02	68.99
48836.1337	6.47	6.46	62.53	62.58	223.5	211.9	63.52	63.46
48868.0447	6.56	6.54	62.06	62.21	200.7	216.3	63.63	63.61
<b>48897.9603</b>	<b>6.61</b>	<b>6.61</b>	<b>61.69</b>	<b>61.86</b>	<b>202.7</b>	<b>218.3</b>	<b>64.22</b>	<b>64.47</b>
48949.8071	6.74	6.72	61.06	61.25	225.3	219.9	67.44	67.36
49006.6367	6.87	6.85	60.36	60.59	243.8	221.6	72.27	72.23
49222.5245	7.29	7.31	58.04	58.08	205.9	227.9	86.52	86.54
49596.9531	8.05	8.06	53.74	53.85	217.0	239.0	63.56	63.45

Table 3. The comparison of the ESOC orbital data with results of the evolution of the improved orbit ( $T_0=48897.960279$ )

T(MJD)	$i$	$\Delta i$	$i_{\Lambda}$	$\Delta i_{\Lambda}$	$\Omega$	$\Delta \Omega$	$\lambda_{\Lambda}$	$\Delta \lambda_{\Lambda}$	$\Delta \lambda_{\Omega}$	
40886.4140	4. <sup>o</sup> 36	0. <sup>o</sup> 00	6. <sup>o</sup> 45	0. <sup>o</sup> 00	282. <sup>o</sup> 9	0. <sup>o</sup> 0	83. <sup>o</sup> 12	0. <sup>o</sup> 00	-	N
48658.0510	10.51	-.09	6.58	-.05	34.6	.2	242.01	1.68	0. <sup>o</sup> 0	E
48668.0000	10.77	.16	6.80	.17	34.5	.2	226.95	5.81	4.17	E
48746.3993	10.75	.02	6.69	.03	33.4	.1	26.83	.33	-0.93	E
48949.5115	11.01	-.02	6.70	-.01	30.9	.1	143.67	.03	-0.24	E
49005.9824	11.13	.02	6.74	.03	30.2	.1	277.90	.00	0.00	E

Table 4. The orbital evolution of GS 67 66C IDSP 3-3 ( $\dot{\lambda}=34.<sup>o</sup>2524/day$ )